Published in final edited form as:
JACC Cardiovasc Imaging. 2013 June ; 6(6): 672–683. doi:10.1016/j.jcmg.2012.09.020.

The Myocardial Extracellular Volume Fraction from T1 Measurements in Healthy Volunteers and Mice; Relationship to Aging and Cardiac Dimensions

Tomas G. Neilan, MD[*,‡], **Otavio R. Coelho-Filho, MD, MPH**[*,&], **Ravi V. Shah, MD**[*,‡], **Siddique A. Abbasi, MD**[*], **Bobak Heydari, MD**[*], **Eri Watanabe, MD, PhD**[¶], **Yucheng Chen**[*], **Damien Mandry, MD**[*], **Francois Pierre-Mongeon**[*,$], **Ron Blankstein, MD**[*], **Raymond Kwong, MD, MPH**[*], and **Michael Jerosch-Herold, PhD**[¶]

[*]Non-invasive Cardiovascular Imaging, Cardiovascular Division, Department of Medicine, Brigham and Women's Hospital

[‡]Division of Cardiology, Department of Medicine, Massachusetts General Hospital

[&]Cardiology Division, School of Medical Science, State University of Campinas (UNICAMP), Campinas, SP, Brazil

[$]Division of Non-invasive Cardiology, Department of Medicine, Montreal Heart Institute, Université de Montréal

[¶]Division of Radiology, Brigham and Women's Hospital, Harvard Medical School

Abstract

Objectives—We aimed to test the characteristics of the myocardial extracellular volume (ECV) fraction derived from pre and post-contrast T1 measurements among healthy volunteers.

Background—Cardiac magnetic resonance (CMR) T1 measurements of myocardium and blood before and after contrast allow quantification of the ECV, a tissue parameter that has been shown to change in proportion to the connective tissue fraction.

Methods—Healthy volunteers underwent a standard CMR with administration of gadolinium. T1 measurements were performed with a Look-Locker sequence followed by gradient-echo acquisition. We tested the segmental, inter-slice, inter-, intra-, and test-retest characteristics of the ECV, as well as the association of the ECV with other variables. Juvenile and aged mice underwent a similar protocol and cardiac sections were harvested for measurement of fibrosis.

Results—In healthy volunteers (n=32, 56% female; ages 21 to 72), the ECV averaged 0.28 ± 0.03 (range 0.23 to 0.33). The intra-class coefficients for the intra-observer, inter-observer, and test-retest absolute agreements of the ECV were 0.94 (95% confidence interval, 0.84 to 0.98), 0.93

Address for correspondence: Michael Jerosch-Herold, Brigham & Women's Hospital, Associate Professor of Radiology, Harvard Medical School, 75 Francis St, Boston, MA 02115. Phone: 617-525-8959; Fax: 617-264-5245; mjerosch-herold@bics.bwh.harvard.edu.

[*]Dr. Neilan and Dr. Coelho-Filho Authors contributed equally to this work.

Disclosures

Dr. Jerosch-Herold is listed as co-inventor on a pending patent application related to detection of diffuse fibrosis by MRI. Otherwise, no other authors have any relevant financial disclosures.

(95% confidence interval, 0.80 to 0.98), and 0.95 (95% confidence interval, 0.52 to 0.99), respectively. In volunteers, the ECV was associated with age (r=0.74, p< 0.001), maximal LA volume index (r=0.67, p< 0.001), and indexed LV mass. There were no differences in the ECV between segments in a slice or between slices. In mice (n=12) the myocardial ECV ranged from 0.20 to 0.32 and increased with age (0.22 ± 0.02 vs. 0.30 ± 0.02, juvenile vs. aged mice, p< 0.001). In mice, the ECV correlated with the extent of myocardial fibrosis (r=0.94, p< 0.001).

Conclusion—In healthy volunteers, the myocardial ECV ranges from 0.23 to 0.33, has acceptable test characteristics, and is associated with age, LA volume, and LV mass. In mice, the ECV also increases with age and strongly correlates with the extent of myocardial fibrosis.

Keywords

Myocardial Fibrosis; Cardiac Magnetic Resonance; T1 measurements; Extracellular Matrix

The presence of focal myocardial fibrosis is associated with adverse cardiovascular outcomes (1–3). Various imaging techniques have emerged to quantify myocardial fibrosis noninvasively. Cardiac magnetic resonance (CMR) with late gadolinium enhancement (LGE) is the current optimal non-invasive technique for detection and quantification of myocardial scar and replacement fibrosis (4). However, limitations exist to LGE-based techniques for detection of diffuse or interstitial myocardial fibrosis. Comparison to pathological standards reveal a marked consistent underestimation of both the presence and the extent of diffuse fibrosis (5–7). The LGE technique relies on relative enhancement of an abnormal region of myocardium in comparison to normal reference. In conditions such as hypertension, sleep apnea, valvular disease, diabetes, obesity, and non-ischemic cardiomyopathy the entire LV may be affected by adverse tissue remodelling, and a normal myocardial reference region may be inappropriately identified. Furthermore, the optimal threshold for quantifying LGE in the presence of diffuse or patchy fibrosis is not well defined (8). These limitations have prompted research into novel CMR-based quantitative techniques for measurement of the myocardial extracellular volume fraction (ECV).

The myocardial ECV increases in proportion to the connective tissue fraction and can be regarded as a continuous measure for the extent of accumulation of myocardial fibrosis (9–11). T1 mapping is a novel CMR-based technique where measured differences in R1 (=1/T1) values before and after gadolinium allow quantification of myocardial ECV (9,12–15). The CMR T1 technique has the potential to differentiate myocardial fibrosis on a continuous scale, from normal myocardium, through diffuse myocardial fibrosis, and ultimately to myocardial scar (16,17). However, limited data exists on the myocardial ECV in a normal healthy population, on the test characteristics of this evolving technique, the optimal CMR protocol for measurement of the myocardial ECV, and on the associations between the ECV and other clinical and imaging variables. Thus, our aims were two-fold. We first wanted to define a normal reference range in a healthy population, as well as define the test characteristics of the myocardial ECV measure. The second aim was to test our hypothesis that the myocardial ECV measure is associated with histological evidence of myocardial fibrosis.

Methods

Study protocol

The protocol was approved by the Partners Healthcare System Human Subjects Review Committee in the Brigham and Women's Hospital (BWH). We recruited healthy volunteer controls by open enrolment. We specifically excluded volunteers with chest pain on exertion, any active or prior history of heart disease, stroke, diabetes, malignancy, sleep

apnea, hypertension, an irregular heart rhythm or atrial fibrillation, or any form of kidney disease. Screening consisted of a comprehensive questionnaire detailing medical and medication history, standard anthropometric data, measurement of blood pressure, pulse, and measurement of serum creatinine and hematocrit.

To determine whether aging was associated with a change in the myocardial ECV in mice and to assess whether aging was associated with a change in the extent of myocardial fibrosis we performed the following protocol in juvenile and aged mice. Juvenile C57BL/6 aged 4 weeks (n = 4) and aged C57BL/6 aged 48 weeks (n = 8) underwent a CMR study. After the CMR study mice were sacrificed and cardiac sections were analyzed for the presence of myocardial fibrosis using Masson's trichrome. Serum hematocrit was recorded on the day of sacrifice immediately after the CMR study. The protocol was approved by the Institutional Animal Care and Use Committee at Harvard University.

Human CMR protocol

All images were acquired with EKG gating, breath-holding, and with the patient in a supine position. Subjects were imaged on 3.0-T CMR system (Tim Trio, Siemens, Erlangen, Germany). The basic CMR protocol consisted of cine steady-state free precession (SSFP) imaging (TR, 3.4 ms; TE, 1.2 ms; in-plane spatial resolution, 1.6 × 2 mm) for LV function and LV mass. Cine imaging was obtained in 8 to 14 matching short-axis (8 mm thick with no gap) and 3 radial long-axis planes. For the calculation of LV mass and function, the endocardial and epicardial borders of the LV myocardium were manually traced on successive short-axis cine images at end-diastole and systole. The papillary muscles were excluded in the LV mass calculation (18), and the LV mass calculation was then indexed to BSA (19). Left atrial systolic and diastolic volumes were measured using the biplane method as previously described (20). All patients underwent an LGE imaging protocol (TR, 4.8 ms; TE, 1.3 ms; inversion time, 200 to 300 ms) to detect focal myocardial fibrosis. A segmented inversion-recovery pulse sequence for LGE was used starting 10–15 minutes after cumulative 0.15-mmol/kg dose of gadolinium DTPA (Magnevist, Bayer HealthCare Pharmaceuticals Inc, Wayne, New Jersey). LGE images were obtained in 8 to 14 matching short-axis (8 mm thick with no gap) and 3 radial long-axis planes.

Human T1 measurements

T1 measurements were performed with a cine Look-Locker sequence, similar to a standard inversion time (TI) scout sequence, with a non-slice-selective adiabatic inversion pulse, followed by segmented gradient-echo acquisition for 17 cardiac phases/times after inversion (TE=2.5 ms; TR = 5.5 ms; flip angle = 10°; 192 × 128 matrix; 6 mm slice), spread over 2 cardiac cycles (sampling frequency of T1 measurements 100 ms pre-contrast, and 55 ms post-contrast, slice thickness 8 mm, TR > 3 RR intervals pre-contrast and 2 RR intervals post-contrast) (12,13,21). The Look-Locker sequence was performed in three short axis slices at the level of the basal, mid, and apical left ventricle. Each sequence was repeated in the same LV short-axis slice, once before and 4 to 5 times after the injection of gadolinium spanning a 30-minute period (Figure 1). Specifically, the initial T1 measure was performed prior to the administration of gadolinium. The second T1 measure was performed 3–4 minutes after the initial dose of contrast (0.05mmol/kg). Immediately after this second T1 measure, a second dose of contrast was given (0.10mmol/kg), as LGE imaging was also performed for completeness. The third T1 measure was performed 3–4 minutes after this second dose of contrast. The final T1 measure was performed just prior to the end of the study, an average of 30–35 minutes after the initial dose of contrast. Either 1 or 2 other T1 measures were performed after the third measure and prior to the final measure at no pre-set intervals.

Mouse CMR protocol

Twelve male C57BL/6 mice were imaged on a Bruker 4.7 T CMR imaging platform. For the CMR study, mice were anesthetized with isofluorane (induction 4–5%; maintenance 1–2% in oxygen from a precision vaporizer). For the CMR study, mice were placed in a special cradle, with EKG electrodes attached with tape to a front and back paw respectively, using electrode gel to optimize contact. For LV volumes and mass, measured after contrast administration, the CMR protocol was built upon an EKG-triggered fast gradient echo FLASH sequence with the following imaging parameters: flip angle 30 degrees, TR, 8.85 ms; TE, 2.36 ms; matrix, spatial resolution, 0.13 × 0.15 mm. Cine imaging was obtained in 8 to 12 matching short-axis (1 mm thick with no gap). LV mass and function was measured in a similar method to the human study. For T1 measurements, we used a Look-Locker sequence with an adiabatic non-slice-selective inversion pulse and the following parameters: flip angle 15°, TR, 2.2 ms; TE, 1.6 ms; in-plane resolution, 0.13 × 0.15 mm, slice thickness 1 mm; 6 ms hyperbolic secant inversion pulse; repetition time per segment: 22 ms; number of averages: 6 (pre-contrast), or 4 (post-contrast). Gadolinium (0.2 mmol/kg) was diluted in saline in a 1:10 ratio and administered by multiple intraperitoneal injections in volumes of 200μL, followed by T1 measurements no earlier than 5 minutes after each injection. Contrast is rapidly (within < 1 minute) taken up in the blood and the myocardium after an intraperitoneal injection, and this avoids the difficulty to obtain tail vein access.

T1 analysis method

For each Look-Locker sequence the endo- and epicardial borders of the LV were traced and divided into 6 standard segments) and segments were numbered 1 through 6 starting from the anterior RV insertion point and proceeding in a clockwise direction (Mass Research, Leiden University Medical Center, The Netherlands, Figure 2). The signal intensity versus time curves for each segment and the blood pool were used to determine segmental T1 through fitting to an analytical expression for the inversion recovery, and correction for the radiofrequency pulse alteration of the inversion recovery. The reciprocal of T1 (R1=1/T1) was used to plot the myocardial R1 against the R1 in the blood pool. Subsequently, the slope of the association was calculated by linear regression, using measurement points with an R1 less than 3 s^{-1}. The slope of the linear relationship (the partition coefficient for gadolinium, λ_{Gd}) was based on an extension of the previously used formula:

$$\lambda_{Gd} = \frac{\Delta R_1(tissue)}{\Delta R_1(blood)} = \frac{R_{1t}^{post} - R_{1t}^{pre}}{R_{1b}^{post} - R_{1b}^{pre}},$$

The above formula, and the linear model apply to the limit of fast transcytolemmal water exchange, and to meet this condition only data points with R1 in blood < 3.0 s^{-1} were used for the linear regression fits. From the slope of this relationship, the myocardial ECV fraction for all 6 myocardial segments was quantified as reported previously (12,13), by multiplying each of the segmental λ_{Gd} by (1-hematocrit in percent/100) (Figure 2). A global myocardial ECV for each healthy volunteer was then calculated by averaging the 6 myocardial segmental values from the mid-LV short axis slice.

Mouse blood pressure measurement

Blood pressure was measured in all mice by tail-cuff manometry using a CODA-3 non-invasive blood pressure monitoring system (Kent Scientific, Torrington, CT). The mice were placed in a plastic tube restrainer, Occlusion and volume-pressure recording cuffs were placed over their tails, and the mice were allowed to adapt to the restrainer for 30 minutes prior to initiating the blood pressure measurement protocol. After the adaptation period,

blood pressure was measured for 5 acclimation cycles followed by 10 measurement cycles. Mice were warmed by heating pads during the acclimation cycles to ensure sufficient blood flow to the tail. The animals were monitored closely throughout the measurement protocol, individually heated or cooled as necessary, and removed from restraint as soon as possible upon completing the measurement protocol. All measurements were taken in the afternoon.

Histological analysis

Hearts from all imaged mice were excised and fixed in formalin-solution for histological analysis. Short axis cuts (~ 1 mm thickness) of formalin fixed tissue were processed and embedded in paraffin using standard histological preparations. Mouse myocardial sections were taken of the entire face of a slice, including septum, left ventricular free wall, and right ventricular wall. The determination of the collagen volume fraction of mice was performed for a mid-level short-axis slice at the same level as the T1 measurement sequences. Sections of approximately 5 microns in thickness were stained with Masson's trichrome and viewed under polarized light using a 20x objective. 15–20 representative areas are chosen in each heart for collagen volume fraction analysis. The Spectrum Analysis algorithm package and ImageScope analysis software (version 9; Aperio Technologies, Inc.) were applied to quantify histochemical staining. The fraction of collagen volume is calculated by counting the number of pixels occupied by the stained region and dividing this count by the number of pixels occupied by the entire section.

Statistical analysis

Continuous data are presented as mean ± SD. Continuous data in mice were compared using an independent Student t-test. Continuous data in humans were compared an ANOVA and corrected using a Bonferroni correction. We assessed the inter- and intra-observer variability in a randomly selected group of 16 volunteers. We also aimed to test the repeatability of the ECV measure when separated by less than 3 months. We measured the test-retest characteristics in 5 randomly selected volunteers by repeating the measurement of the myocardial ECV within 1 month. Comparison of the inter-observer and intra-observer characteristics of the myocardial ECV were made using Bland-Altman plots and determination of the 95% limits of agreement between methods. We determined the intra-class correlation coefficients for the inter-observer, intra-observer, and test-retest absolute agreements of the ECV. To test whether the addition of multiple post-contrast measures of T1 could reduce the variability of the ECV measure, we compared the variances of the ECV when measured using a single post-contrast T1 and three post-contrast T1 values, in combination with a pre-contrast T1 value (for both cases). Comparison of the standard deviations of ECV from a single post-contrast T1 and the ECV from 3 post-contrast T1 measures was made using an F-statistic. We also determined the association between the myocardial ECV and other cohort characteristics using a Pearson correlation. We performed a multivariable analysis in humans of the ECV vs. age, body surface area, LV mass, and heart rate. The Akaike Information Criterion (AIC) was used as the criterion for selection of the best prognostic model for a level of significance of 0.05 (22). A two-sided p value of < 0.05 was deemed significant. Regression analysis was performed in R-statistics software (version 2.9.0); SAS was used for all other statistical analysis (SAS Institute Inc, Cary).

Results

Baseline parameters in healthy volunteers

Overall, 32 volunteers were recruited and all were included in the analysis. There were 18 women (56%) and 14 men. The mean age of volunteers was 49 ± 15 years, with a range from 21 to 72 years. The average body mass index was 26 ± 6 kg/m^2, systolic blood

pressure was 120 ± 11 mmHg, diastolic blood pressure was 74 ± 7 mmHg, heart rate was 68 ± 11 beats per min, and hematocrit was 42 ± 3% (Table 1).

Baseline CMR parameters in healthy volunteers

Baseline CMR parameters are presented in Table 1. In brief, mean left ventricular (LV) end diastolic volume (EDV) was 133 ± 29 mls, indexed LV mass was 45 ± 7 grams/m^2, right ventricular (RV) EDV was 131 ± 31 mls, indexed maximal left atrial (LA) volume was 33 ± 10 mls/m^2, RV ejection fraction (EF) 53 ± 4 %, and LVEF 64 ± 7 %.

Myocardial extracellular volume fraction in healthy volunteers

Late gadolinium enhancement was not identified in any normal volunteer. The number of R1 measurements of < 3.0 s^{-1} ranged from 3 to 4 (mean 3.5) in all human studies. We measured the myocardial ECV in 6 segments in three slices of the LV (basal, mid-ventricular and apical). The average myocardial ECV was 0.28 ± 0.03 (range 0.23 to 0.33). There was no difference in the myocardial ECV between basal, mid or apical slices in healthy controls (0.27 ± 0.02 vs. 0.28 ± 0.03 vs. 0.28 ± 0.03, basal, mid and apical slices respectively, p = 0.34 for trend). There was also no difference between segments within a slice, for example the mid-ventricle was split into 6 segments (0.28 ± 0.04, 0.28 ± 0.04, 0.28 ± 0.04, 0.29 ± 0.04, 0.29 ± 0.03, 0.30 ± 0.03, segments 1 through 6 respectively, p = 0.38 for trend). We measured the inter- and intra-observer variability in 15 randomly selected studies. The mean inter-observer difference was 0.02 ± 0.01 (95% CI −0.005 to 0.005, Figure 3A), the mean intra-observer difference was 0.01 ± 0.01 (95% CI −0.005 to 0.005, Figure 3B) and the test-retest difference was 0.01 ± 0.01 (95% CI −0.015 to 0.015). The intra-class coefficients for the intra-observer, inter-observer, and the test-retest measurements of the ECV were 0.94 (n=16, 95% confidence interval, 0.84 to 0.98), 0.93 (n= 16, 95% confidence interval, 0.80 to 0.98), and 0.95 (n=5, 95% confidence interval, 0.52 to 0.99), respectively. The cohort was separated according to gender. The groups did not differ in age (51 ± 14 years vs. 47 ± 15 years, p= 0.30). There were no difference in the myocardial ECV in males as compared to females (0.28 ± 0.03 vs. 0.27 ± 0.03, males vs. females, p = 0.20). To test whether the use of multiple T1 measures post-contrast reduced measurement variability, we compared the measurement variability of the ECV using a single T1 measure as compared to using 3 post-contrast T1 measures. We found using a single measure was associated with a higher standard deviation of 0.041, than using three post-contrast T1 measures which had a standard deviation of 0.026 (p = 0.02).

Association between the ECV and other variables in healthy volunteers

The myocardial ECV increased with age (r=0.74, p < 0.001). To test the presence of confounders, we tested the association between pre-contrast blood pool T1 values and heart rate and age. There was no association between the heart rate and the ECV (r=−0.02) and age and pre-contrast blood pool T1 values (r=−0.09). We performed a multivariable analysis for the ECV vs. age, body surface area, LV mass, and the heart rate. Using this we got a final multivariable model of the following in which age had the strongest independent association with the ECV (t value 6.00, p < 0.0001). The entire cohort was split into three age ranges of < 40, 40–60, and > 60 years of age. There was a graded increase in the myocardial ECV from 0.25 ± 0.02 vs. 0.27 ± 0.03 vs. 0.31 ± 0.02 with increasing age ranges (p < 0.001, Figure 4A). There was no association between the myocardial ECV and heart rate (r=−0.07). There was an association between the myocardial ECV and indexed LV mass (r=0.52, p < 0.01, Figure 4B) and maximal LA volume index (r=0.67, p < 0.001).

Comparison between Juvenile and Aged Mice

As expected, body weight, LV volumes, LV mass and stroke volumes were increased in aged mice as compared to juvenile mice (Table 2) (23). Both the systolic and diastolic blood pressure was unchanged in juvenile as compared to aged mice. The myocardial ECV was higher in older as compared to younger mice (0.22 ± 0.02 vs. 0.30 ± 0.02, juvenile vs. aged, $p < 0.001$, Figure 5A). Hearts were harvested immediately after the CMR study and sections were stained using Masson's trichrome. There was an increase in myocardial fibrosis in aged mice in comparison to juvenile mice (2.1 ± 1 vs. 5.8 ± 1 %, young vs. old mice, $p < 0.001$). There was a strong association between the myocardial ECV and LV mass ($r=0.81$, $p < 0.001$) and the extent of myocardial fibrosis ($r=0.93$, $p < 0.001$, Figure 5B). Representative images are shown from a juvenile and aged mouse (Figure 5C–F).

Discussion

In this study we measured the myocardial ECV in healthy volunteers and mice using a quantitative T1 technique. The myocardial ECV averaged 0.28 ± 0.03 and ranged from 0.23 to 0.33 in humans. In humans, there was a correlation between myocardial ECV, age, and LV mass. Importantly, there was a consistent increase in the myocardial ECV with increasing age in both volunteers and mice. In mice, we were able to test whether the increase in the myocardial ECV with age was associated with expansion of the extracellular matrix. In mice, there was a strong association between the increase in the myocardial ECV and histological evidence of increasing myocardial fibrosis. The range of myocardial ECV in mice was similar to the range observed in our human volunteers. These data suggest that aging is associated with an increase in the myocardial extracellular volume that is detectable using T1 measurements.

These data on non-invasive quantification of the myocardial ECV are both additive to and an extension of previously published work (9,12–15,24–26). Klein and colleagues used a Look-Locker sequence to calculate a volume of distribution of gadolinium, an ECV, in patients with an ischemic cardiomyopathy. They found that the ECV was elevated in areas of scar compared to "normal" myocardium (25). Lee and colleagues measured myocardial T1 values at 3T in normal healthy volunteers using a different technique (modified lock locker inversion recovery technique, MOLLI) and calculated an average ECV of 27%. Some differences exist between methods employed in this and previous studies. Firstly, because we rely on the change of R1 with time, and not on absolute T1 or R1 values, the results are relatively independent of field strength. The technique adjusts for the blood levels of gadolinium by relating the change of R1 in the myocardium and to the corresponding R1 change in blood. Therefore, the estimate of ECV is gadolinium dose-independent, and largely independent of the clearance of gadolinium from the blood pool, as proven by a previous comparison of the infusion and bolus techniques for ECV quantification (21). The Look-Locker technique used here for T1 imaging allows image acquisition within a single breath-hold per slice, while maintaining a TI resolution of 50 ms for post-contrast measurements acquisition. The protocol employed, with at least 3 post-contrast T1 measurements at 3 slice levels, extends a regular CMR study by 5–10 minutes. This method does not depend on the exact timing of the T1 measurement after infusion of gadolinium as multiple measurements of T1 times are recorded, repeated multiple times over the course of the CMR study to optimize the accuracy of the partition coefficient determination. A previous report on the measurement of the partition coefficient for gadolinium contrast in human myocardium (λ_{Gd}), noted a relatively large range for λ_{Gd}, corresponding to a 50–60% change of ECV, assuming a constant Hct (21). The adjustment of the partition co-efficient for gadolinium by multiplication with (1-hematocrit) to determine the myocardial extracellular volume fraction may be one reason for the reduced variability in this study (21). Furthermore, more than two T1 measurements were used in combination with a linear

regression fit for all values with R1 in blood < 3.0 s^{-1}, which reduces variability compared to a two-point method.

This work has potential clinical and research implications. Aging is associated with a progressive increase in ventricular stiffness and impaired diastolic function (27,28). This age-related impairment of diastolic function is associated with the development of heart failure and increased mortality (29,30). Similar to published data in patients with known or suspected cardiovascular disease (14), we found that age was associated with an increase in the myocardial ECV in healthy human volunteers in this study. Key differences may relate to the study cohort. We specifically selected healthy subjects free of cardiovascular disease, hypertension, diabetes, and sleep apnea, with a normal blood pressure, and a structurally normal heart. However, data are conflicting regarding the relationship between the ECV and age, and the association between the ECV and LV mass (31). We note that in our study there is a significant positive correlation between ECV and LV mass, but in a multivariate regression model for the ECV, there was no significant association between ECV and LV mass, if ECV is simultaneously adjusted by age and gender, suggesting that the association between the ECV and LV mass may be confounded by age. While limited data exist regarding the association between the ECV and LV mass, there are significant supportive data detailing the strong association between myocardial fibrosis as measured using LGE-based techniques and increased LV mass (32,33). We also show, in wild-type mice, the pathological correlative finding of an increase in myocardial fibrosis. These mice data are consistent with published animal work demonstrating an associated with aging and myocardial fibrosis (34,35). Human pathological data are conflicting but significant supportive data exist suggesting that aging is associated with expansion of the extracellular space, and an increase in interstitial fibrosis and appearance of small foci of replacement fibrosis in men and women (36–38). Apoptosis, an enlargement of myocyte size, and extra-cellular matrix proliferation are other distinctive, age-associated changes in myocardial structure. Measurement of the myocardial extracellular volume may provide an early marker of these adverse changes in myocardial tissue structure and may precede overt impairment of ventricular function. To support this, we also found an association between the myocardial ECV and left atrial volume, the latter a commonly-used index of diastolic function. However, further work will help determine the natural progression of changes in myocardial structure and function, and whether the CMR-detected increase in the myocardial ECV is associated with an increased risk for heart failure.

A robust marker for expansion of the extracellular volume may have extended applicability in cardiovascular monitoring (39). Prior work has reported a similar normal range for myocardial ECV (14,26), and has shown that the ECV can reliably differentiate between normal and abnormal myocardium (14,25). Flett and colleagues tested whether serial T1 measures were an index of pathological expansion of the extracellular space. In that study, they found a strong association between the ECV and the extent of myocardial fibrosis in patients with aortic stenosis and hypertrophic cardiomyopathy (9). Finally, Iles and colleagues found that post-contrast T1 correlated with histological evidence of myocardial fibrosis in patients with heart failure and extended these finding by showing an association with diastolic function (10). By contrast, the present study focused on a cohort of volunteers without any previous history, or signs or symptoms of cardiac disease.

This study has to be interpreted within the context of the design format. Image acquisition only extends an average clinical study by 5 minutes; however, the interpretation currently requires manual tracing of the endocardial contours for 16–17 phases from a cine image at up to five time points. We performed a total of 4–5 T1 measures, a pre-gadolinium measure and 3–4 post-gadolinium measures after a cumulative dose of gadolinium of 0.15mmol/kg. However, unlike standard clinical practice, the dose of gadolinium was split. While we

acknowledge this as a limit to the external application, we do not believe that this would likely yield a significant difference in the ECV as compared to a single-dose of gadolinium. Pathological validation for the myocardial ECV as a biomarker for the extracellular volume fraction has been published (9); We did not perform endomyocardial biopsies in our healthy volunteer population or provide serum surrogates for collagen turnover. To attempt to address this limitation, we tested the myocardial ECV in mice and found that, similar to humans, there was an age-related increase in the myocardial ECV. However, important biological differences have been reported regarding the effect of aging in rodents as compared to humans which we did not address (40). Other techniques are also available for measuring myocardial T1. These techniques include the modified Look-Locker inversion recovery (MOLLI) and the shortened modified Look-Locker Inversion recovery (ShMOLLI) method. Techniques such as MOLLI and ShMOLLI are acquired in the same quiescent window of several cardiac cycles as opposed to data acquisition over the entire cardiac cycle of the Look-Locker cine sequence used in this study. Also, while the acquisition time for the raw data is similar between ShMOLLI and the Look-locker sequence, the analysis time is faster for either the ShMOLLI or the MOLLI method (15,41). Data from Kawel and colleagues using the MOLLI technique with Gd-DTPA and Gd-BOPTA have shown that the relaxivity of the contrast agent may play a role in the ECV determination (24). It is known that the relaxivity of Gd-BOPTA depends of protein concentration, a property that can be potentially a confounding factor in the determination of the extracellular volume fraction. We did not perform echocardiography in healthy controls to determine whether or not an association existed between measures of diastolic function and the myocardial ECV. Furthermore, while all controls were free of cardiovascular disease by history, had a normal blood pressure, and had a structurally normal heart on CMR imaging, we did not perform a 12-lead EKG to further add to this assessment. However, we did find an association between the myocardial ECV and left atrial volume with an increase in the ECV being associated with larger left atrial volume suggesting a potential link. Multiple pathological processes such as edema and infiltration can expand the extracellular matrix and measurement of the myocardial ECV alone is unable to differentiate between these processes, and hence has to be interpreted within a clinical context.

In summary, the ECV is a novel and potentially useful index for quantification of the myocardial extracellular volume fraction. In humans, the myocardial ECV increases with age, is associated with LV mass and LA volume, and has reliable test characteristics. In mice, the myocardial ECV also increases with age, is also associated with LV mass, and is strongly associated with the extent of myocardial fibrosis. Further work will need to be done to test the application of this technique to patients with cardiovascular disease associated with the development of myocardial fibrosis.

Acknowledgments

Sources of Funding

Dr. Neilan is supported by an American Heart Association Fellow to Faculty grant (12FTF12060588) and previously by an NIH T32 Training Grant (T32HL09430101A1). Dr. Mongeon receives financial support for research from the Montreal Heart Institute Foundation, Montreal, Canada. Dr. Kwong receives salary support from a research grant from the National Institutes of Health (R01HL091157).

Dr. Jerosch-Herold is supported in part by a research grant from the National Institutes of Health (R01HL090634-01A1).

We thank our CMR technologists for continued excellence.

Abbreviations

CMR	cardiac magnetic resonance
LGE	late gadolinium enhancement
EF	ejection fraction
AC	anthracyclines
ECV	Myocardial extracellular volume fraction
ECM	Myocardial extracellular matrix

References

1. Assomull RG, Prasad SK, Lyne J, et al. Cardiovascular magnetic resonance, fibrosis, and prognosis in dilated cardiomyopathy. J Am Coll Cardiol. 2006; 48:1977–85. [PubMed: 17112987]
2. Dweck MR, Joshi S, Murigu T, et al. Midwall fibrosis is an independent predictor of mortality in patients with aortic stenosis. J Am Coll Cardiol. 2011; 58:1271–9. [PubMed: 21903062]
3. Kwong RY, Chan AK, Brown KA, et al. Impact of unrecognized myocardial scar detected by cardiac magnetic resonance imaging on event-free survival in patients presenting with signs or symptoms of coronary artery disease. Circulation. 2006; 113:2733–43. [PubMed: 16754804]
4. Kim RJ, Fieno DS, Parrish TB, et al. Relationship of MRI delayed contrast enhancement to irreversible injury, infarct age, and contractile function. Circulation. 1999; 100:1992–2002. [PubMed: 10556226]
5. Azevedo CF, Nigri M, Higuchi ML, et al. Prognostic significance of myocardial fibrosis quantification by histopathology and magnetic resonance imaging in patients with severe aortic valve disease. J Am Coll Cardiol. 2010; 56:278–87. [PubMed: 20633819]
6. Mewton N, Liu CY, Croisille P, Bluemke D, Lima JA. Assessment of myocardial fibrosis with cardiovascular magnetic resonance. J Am Coll Cardiol. 2011; 57:891–903. [PubMed: 21329834]
7. Schalla S, Bekkers SC, Dennert R, et al. Replacement and reactive myocardial fibrosis in idiopathic dilated cardiomyopathy: comparison of magnetic resonance imaging with right ventricular biopsy. Eur J Heart Fail. 2010; 12:227–31. [PubMed: 20156939]
8. Flett AS, Hasleton J, Cook C, et al. Evaluation of techniques for the quantification of myocardial scar of differing etiology using cardiac magnetic resonance. JACC Cardiovasc Imaging. 2011; 4:150–6. [PubMed: 21329899]
9. Flett AS, Hayward MP, Ashworth MT, et al. Equilibrium contrast cardiovascular magnetic resonance for the measurement of diffuse myocardial fibrosis: preliminary validation in humans. Circulation. 2010; 122:138–44. [PubMed: 20585010]
10. Iles L, Pfluger H, Phrommintikul A, et al. Evaluation of diffuse myocardial fibrosis in heart failure with cardiac magnetic resonance contrast-enhanced T1 mapping. J Am Coll Cardiol. 2008; 52:1574–80. [PubMed: 19007595]
11. Arheden H, Saeed M, Higgins CB, et al. Measurement of the distribution volume of gadopentetate dimeglumine at echo-planar MR imaging to quantify myocardial infarction: comparison with 99mTc-DTPA autoradiography in rats. Radiology. 1999; 211:698–708. [PubMed: 10352594]
12. Broberg CS, Chugh SS, Conklin C, Sahn DJ, Jerosch-Herold M. Quantification of diffuse myocardial fibrosis and its association with myocardial dysfunction in congenital heart disease. Circ Cardiovasc Imaging. 2010; 3:727–34. [PubMed: 20855860]
13. Jerosch-Herold M, Sheridan DC, Kushner JD, et al. Cardiac magnetic resonance imaging of myocardial contrast uptake and blood flow in patients affected with idiopathic or familial dilated cardiomyopathy. Am J Physiol Heart Circ Physiol. 2008; 295:H1234–H1242. [PubMed: 18660445]
14. Ugander M, Oki AJ, Hsu LY, et al. Extracellular volume imaging by magnetic resonance imaging provides insights into overt and sub-clinical myocardial pathology. Eur Heart J. 2012; 54:127–145.

15. Messroghli DR, Radjenovic A, Kozerke S, Higgins DM, Sivananthan MU, Ridgway JP. Modified Look-Locker inversion recovery (MOLLI) for high-resolution T1 mapping of the heart. Magn Reson Med. 2004; 52:141–6. [PubMed: 15236377]
16. Thornhill RE, Prato FS, Wisenberg G, White JA, Nowell J, Sauer A. Feasibility of the single-bolus strategy for measuring the partition coefficient of Gd-DTPA in patients with myocardial infarction: independence of image delay time and maturity of scar. Magn Reson Med. 2006; 55:780–9. [PubMed: 16508912]
17. Thornhill RE, Prato FS, Wisenberg G, Moran GR, Sykes J. Determining the extent to which delayed-enhancement images reflect the partition-coefficient of Gd-DTPA in canine studies of reperfused and unreperfused myocardial infarction. Magn Reson Med. 2004; 52:1069–79. [PubMed: 15508150]
18. Rickers C, Wilke NM, Jerosch-Herold M, et al. Utility of cardiac magnetic resonance imaging in the diagnosis of hypertrophic cardiomyopathy. Circulation. 2005; 112:855–61. [PubMed: 16087809]
19. Flacke SJ, Fischer SE, Lorenz CH. Measurement of the gadopentetate dimeglumine partition coefficient in human myocardium in vivo: normal distribution and elevation in acute and chronic infarction. Radiology. 2001; 218:703–10. [PubMed: 11230643]
20. Farzaneh-Far A, Ariyarajah V, Shenoy C, et al. Left atrial passive emptying function during dobutamine stress MR imaging is a predictor of cardiac events in patients with suspected myocardial ischemia. JACC Cardiovasc Imaging. 2011; 4:378–88. [PubMed: 21492813]
21. Schelbert EB, Testa SM, Meier CG, et al. Myocardial extravascular extracellular volume fraction measurement by gadolinium cardiovascular magnetic resonance in humans: slow infusion versus bolus. J Cardiovasc Magn Reson. 2011; 13:16. [PubMed: 21375743]
22. Venables, W.; Ripley, B. Modern Applied Statistics with S. 4. Springer; 2002.
23. Wiesmann F, Ruff J, Hiller KH, Rommel E, Haase A, Neubauer S. Developmental changes of cardiac function and mass assessed with MRI in neonatal, juvenile, and adult mice. Am J Physiol Heart Circ Physiol. 2000; 278:H652–7. [PubMed: 10666098]
24. Kawel N, Nacif M, Zavodni A, et al. T1 mapping of the myocardium: Intra-individual assessment of the effect of field strength, cardiac cycle and variation by myocardial region. J Cardiovasc Magn Reson. 2012; 14:27. [PubMed: 22548832]
25. Klein C, Nekolla SG, Balbach T, et al. The influence of myocardial blood flow and volume of distribution on late Gd-DTPA kinetics in ischemic heart failure. J Magn Reson Imaging. 2004; 20:588–93. [PubMed: 15390232]
26. Lee JJ, Liu S, Nacif MS, et al. Myocardial T1 and extracellular volume fraction mapping at 3 tesla. J Cardiovasc Magn Reson. 2011; 13:75. [PubMed: 22123333]
27. Benjamin EJ, Levy D, Anderson KM, et al. Determinants of Doppler indexes of left ventricular diastolic function in normal subjects (the Framingham Heart Study). Am J Cardiol. 1992; 70:508–15. [PubMed: 1642190]
28. Martos R, Baugh J, Ledwidge M, et al. Diastolic heart failure: evidence of increased myocardial collagen turnover linked to diastolic dysfunction. Circulation. 2007; 115:888–95. [PubMed: 17283265]
29. Bursi F, Weston SA, Redfield MM, et al. Systolic and diastolic heart failure in the community. Jama. 2006; 296:2209–16. [PubMed: 17090767]
30. Redfield MM, Jacobsen SJ, Burnett JC Jr, Mahoney DW, Bailey KR, Rodeheffer RJ. Burden of systolic and diastolic ventricular dysfunction in the community: appreciating the scope of the heart failure epidemic. Jama. 2003; 289:194–202. [PubMed: 12517230]
31. Sado DM, Flett AS, Banypersad SM, et al. Cardiovascular magnetic resonance measurement of myocardial extracellular volume in health and disease. Heart. 2012
32. Rudolph A, Abdel-Aty H, Bohl S, et al. Noninvasive detection of fibrosis applying contrast-enhanced cardiac magnetic resonance in different forms of left ventricular hypertrophy relation to remodeling. J Am Coll Cardiol. 2009; 53:284–91. [PubMed: 19147047]
33. Moon JC, Mogensen J, Elliott PM, et al. Myocardial late gadolinium enhancement cardiovascular magnetic resonance in hypertrophic cardiomyopathy caused by mutations in troponin I. Heart. 2005; 91:1036–40. [PubMed: 16020591]

34. Derumeaux G, Ichinose F, Raher MJ, et al. Myocardial alterations in senescent mice and effect of exercise training: a strain rate imaging study. Circ Cardiovasc Imaging. 2008; 1:227–34. [PubMed: 19808547]

35. Eghbali M, Eghbali M, Robinson TF, Seifter S, Blumenfeld OO. Collagen accumulation in heart ventricles as a function of growth and aging. Cardiovasc Res. 1989; 23:723–9. [PubMed: 2598224]

36. Olivetti G, Melissari M, Capasso JM, Anversa P. Cardiomyopathy of the aging human heart. Myocyte loss and reactive cellular hypertrophy. Circ Res. 1991; 68:1560–8. [PubMed: 2036710]

37. Gazoti Debessa CR, Mesiano Maifrino LB, Rodrigues de Souza R. Age related changes of the collagen network of the human heart. Mech Ageing Dev. 2001; 122:1049–58. [PubMed: 11389923]

38. Barasch E, Gottdiener JS, Aurigemma G, et al. Association between elevated fibrosis markers and heart failure in the elderly: the cardiovascular health study. Circ Heart Fail. 2009; 2:303–10. [PubMed: 19808353]

39. Ho CY, Lopez B, Coelho-Filho OR, et al. Myocardial fibrosis as an early manifestation of hypertrophic cardiomyopathy. N Engl J Med. 363:552–63. [PubMed: 20818890]

40. Zhang XP, Vatner SF, Shen YT, et al. Increased apoptosis and myocyte enlargement with decreased cardiac mass; distinctive features of the aging male, but not female, monkey heart. J Mol Cell Cardiol. 2007; 43:487–91. [PubMed: 17720187]

41. Piechnik SK, Ferreira VM, Dall'Armellina E, et al. Shortened Modified Look-Locker Inversion recovery (ShMOLLI) for clinical myocardial T1-mapping at 1. 5 and 3 T within a 9 heartbeat breathhold. J Cardiovasc Magn Reson. 2010; 12:69. [PubMed: 21092095]

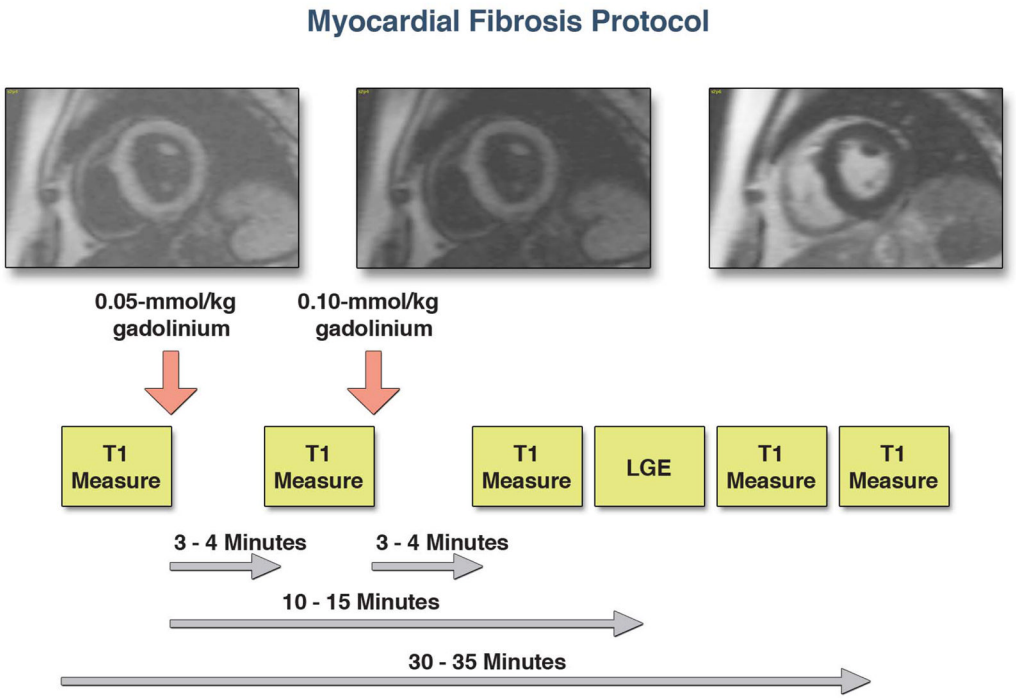

Figure 1.
We used the following protocol for myocardial fibrosis imaging. For the myocardial ECV measurement, images were acquired pre-contrast and up to 4–5 time points post-contrast after a total of 0.15 mmol/kg of gadolinium. LGE imaging was performed starting 10–15 minutes after administration of gadolinium.

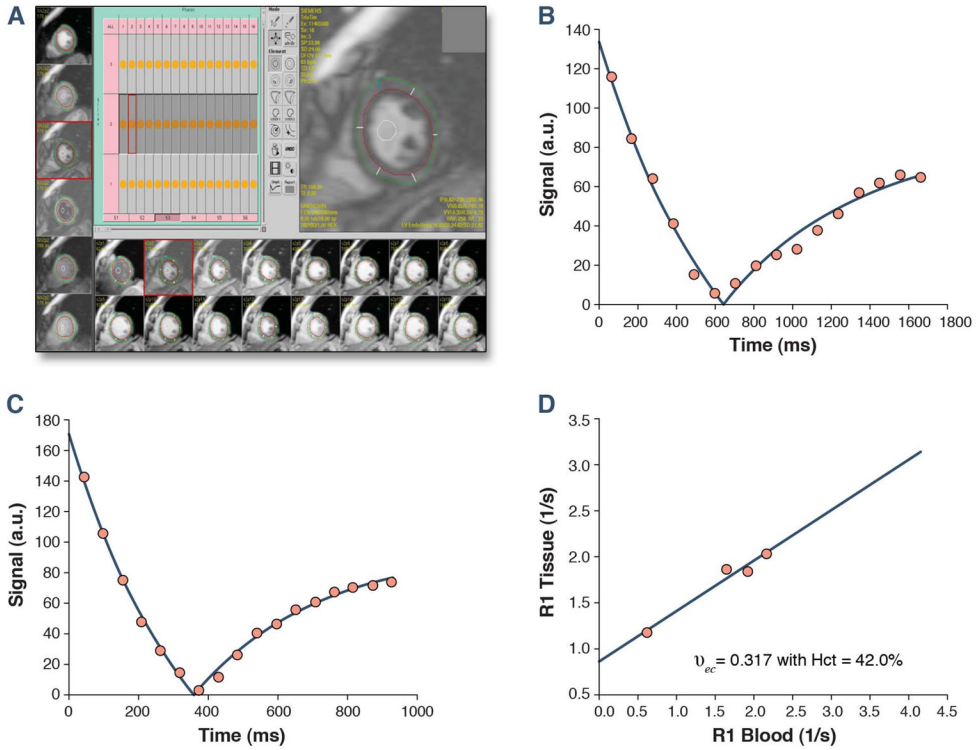

Figure 2.

For each phase of each slice the endo- and epicardial borders of the LV were traced and divided into 6 standard segments. This was repeated for 1 time-point pre-gadolinium and 4–5 time-points post-gadolinium. A further region of interest was drawn in the LV cavity. Segments were then annotated 1 through 6 starting from the anterior RV insertion point and proceeding in a clockwise direction (A). Representative curves for the inversion time pre (B) and post gadolinium (C) are shown, displaying shortening of the inversion time. The myocardial extracellular volume fraction for this representative healthy volunteer (aged 72 years, ECV index of 0.32) is then derived by fitting of the R1 (1/T1) in the myocardium vs. the blood and with adjustment for the serum hematocrit (D).

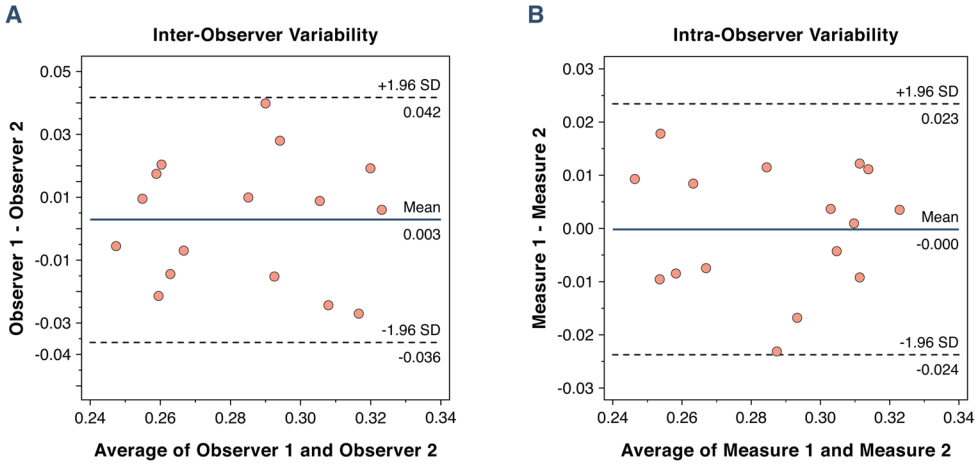

Figure 3.
Bland-Altman plots showing the 95% limits of agreement between two observers (A) and within a single observer (B) for 15 randomly selected volunteers.

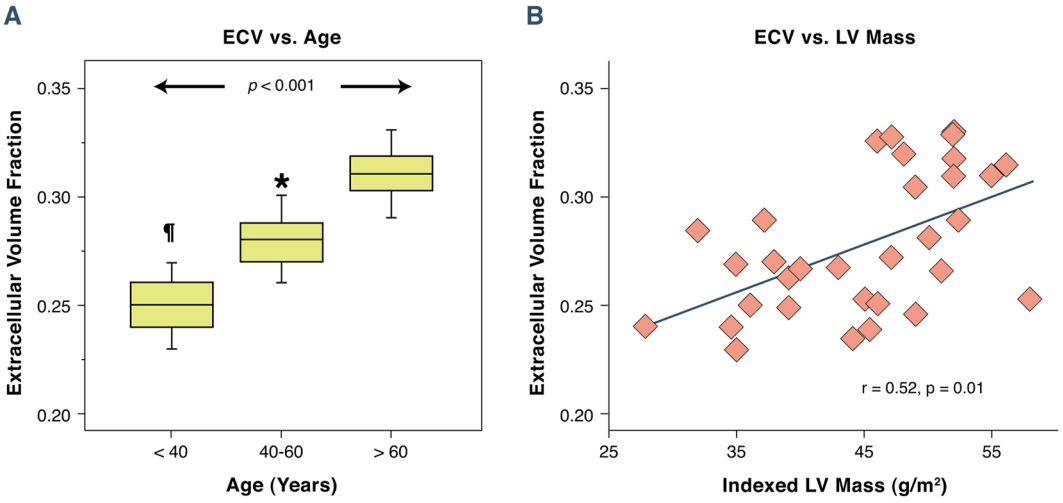

Figure 4.

Association between the myocardial ECV and age in healthy volunteers: There was a strong association between the myocardial ECV and age (A), and the ECV with indexed LV mass (B).

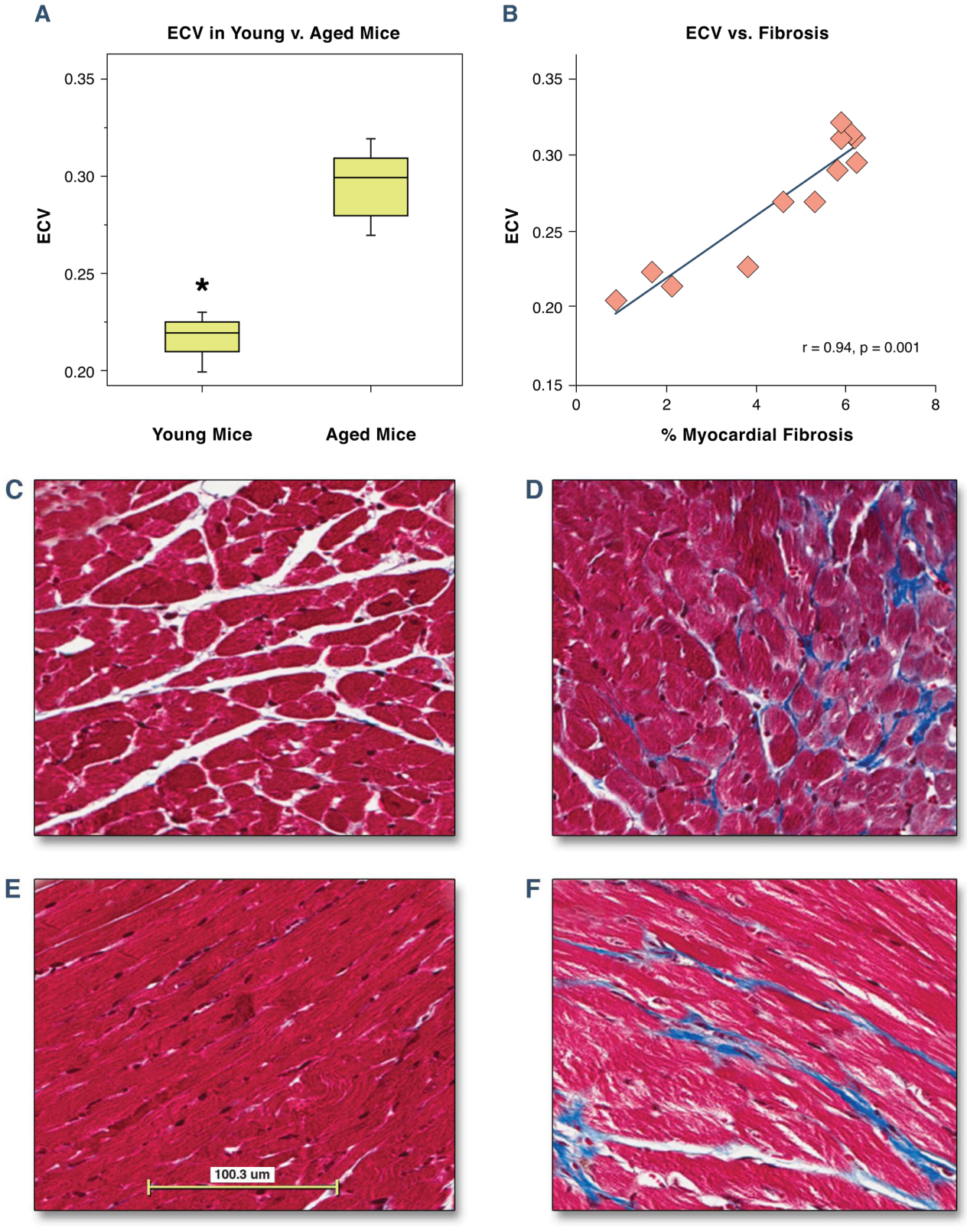

Figure 5.

The myocardial ECV in juvenile and aged mice. Juvenile (4 weeks) and aged mice (48 weeks) underwent a CMR study. After the CMR study mice were euthanized and cardiac sections were harvested for measurement of myocardial fibrosis using Masson's trichrome. The myocardial ECV was higher in aged mice than juvenile mice (0.22 ± 0.02 vs. 0.30 ± 0.02, $p < 0.001$, 4A). Histological analysis revealed an increase in the extent of myocardial fibrosis in young vs. older mice (2.1 ± 1 vs. 5.8 ± 1 %, young vs. old mice, $p < 0.001$). There was a strong association between the myocardial ECV and the extent of myocardial fibrosis ($r=0.93$, $p < 0.001$, 4B). Representative images are shown from a juvenile mouse (4C and 4E) and an aged mouse (4D and 4F) showing normal myocardial architecture stained in red with interwoven patches of myocardial fibrosis stained green.

Table 1

Patient Characteristics and CMR Variables Grouped by Tertiles of Age

	Cohort (32)	Age < 40 (10)	Age 40–60 (11)	Age > 60 (11)	p Value
Mean Age (yrs)	49 (15)	31 (7)	51 (5)	65 (5)	<0.001
Female (number, %)	17 (56)	5 (50)	6 (55)	7 (70)	0.23
Body Mass Index (kg/m^2)	26 (6)	24 (4)	28 (6)	27 (6)	0.27
Systolic Blood Pressure (mmHg)	120 (11)	111 (11)	121 (11)	125 (6)	0.31
Diastolic Blood Pressure (mmHg)	74 (7)	72 (5)	72 (8)	74 (5)	0.72
Heart Rate (beats/minute)	68 (11)	63 (13)	68 (8)	68 (9)	0.56
LVEDV (ml)	133 (24)	142 (23)	141 (20)	118 (27)	0.12
LVESV (ml)	48 (15)	50 (17)	51 (9)	43 (15)	0.24
Septal Wall Thickness (mm)	8 (1)	6 (1)	7 (1)	8 (1)	0.24
Lateral Wall Thickness (mm)	7 (1)	7 (1)	7 (1)	7 (1)	0.24
LV Mass Index (g/m^2)	45 (7)	41 (9)	46 (4)	47 (8)	0.23
RVEDV (ml)	131 (31)	154 (27)	138 (24)	113 (25)	0.009
RVESV (ml)	61 (10)	76 (8)	59 (8)	55 (11)	0.015
Indexed Max LA Volume (ml/m^2)	33 (10)	29 (9)	33 (10)	37 (8)	0.12
LVEF (%)	64 (7)	64 (9)	64 (14)	63 (7)	0.66
RVEF (%)	53 (4)	51 (5)	56 (7)	51 (5)	0.53
ECV	0.28 (0.03)	0.25 (0.02)	0.27 (0.03)	0.31 (0.02)	<0.001

All data are mean (SD) unless otherwise indicated; LVEDV = left ventricular end diastolic volume; LVESV = left ventricular end systolic volume; RVEDV = right ventricular end diastolic volume; RVESV = right ventricular end systolic volume; LVEF = left ventricular ejection fraction; RVEF = right ventricular ejection fraction; ECV = myocardial extracellular volume fraction derived from quantitative T1 measurements;

Table 2

Mouse Characteristics and CMR Variables

	Age 4 Weeks (n=4)	Age 48 Weeks (n=8)	p Value
Body Weight (grams)	20 (1)	38 (2)	<0.001
Heart Rate (BPM)	496 (41)	455 (44)	0.14
Systolic Blood Pressure (mmHg)	109 (4)	114 (4)	0.08
Diastolic Blood Pressure (mmHg)	80 (4)	81 (3)	0.60
LVEDV (ml)	40 (9)	70 (8)	<0.001
LVESV (ml)	12 (5)	25 (4)	<0.001
LV Mass (mg)	57 (4)	119 (16)	<0.001
LVEF (%)	70 (5)	64 (6)	0.09
Cardiac Output (mls/min)	14 (2)	16 (4)	0.22
Stroke Volume (mls)	31 (9)	45 (8)	0.02
ECV	0.22 (0.02)	0.30 (0.02)	<0.001

All data are mean (SD) unless otherwise indicated; LVEDV = left ventricular end diastolic volume; LVESV = left ventricular end systolic volume; LVEF = left ventricular ejection fraction; ECV = myocardial extracellular volume fraction derived from quantitative T1 measurements